

Sorption of thorium from aqueous solutions onto natural and modified zeolites

Filippos Karantoumanis, Fotini Noli

*Radiochemical Laboratory of the General & Inorganic Chemistry Department, School of Chemistry,
Aristotle University, Thessaloniki, 54124 Greece*

Corresponding author: noli@chem.auth.gr

DOI: 10.62579/JAGC0016

Abstract

A natural HEU-type zeolite from Greece was embedded with iron oxyhydroxides via a simple and fast precipitation method following acid pretreatment. The raw and modified materials were subsequently evaluated as sorbents for thorium removal from acidic aqueous solutions. Surface techniques (BET, pH_{pzc}) and structural characterization methods such as Fourier Transform Infrared Spectroscopy (FTIR) and X-Ray Diffraction (XRD) were implemented for both materials before and after metal sorption. The experimental results were used for the construction of sorption isotherms while the data were also fitted using mathematical models for a brief insight into the sorption mechanism accompanied by kinetic and thermodynamic studies. Results showed that the modification process caused changes in the characteristics of the precursor material and that thorium uptake was greatly affected by the presence of iron oxyhydroxides.

Keywords Zeolites; Fe-oxyhydroxides; thorium; sorption; isotherms

INTRODUCTION

Thorium is one of the most commonly occurring actinides in the Earth's crust, forming a variety of compounds with many elements. Among others such as thorianite (ThO_2), thorite, and uranothorite, monazite is the most important commercially exploitable mineral, and often a common by-product of ore mining. However, thorium does not exhibit the complex aqueous chemistry of other actinides like uranium. It is present in nature only in the 4+ oxidation state, Th(IV), and most of its complexes with common ligands have very low solubility. As a result, its concentration in natural waters is significantly lower [1, 2].

Nonetheless, thorium is an important waste produced by ore mining and milling operations that can contaminate ground- and surface water deposits, posing a threat to the ecosystem and humans. Exposure to high concentrations of thorium, although rare, can lead to serious health issues due to its chemical toxicity, including organ failure, respiratory problems, or even cancer [3, 4].

Among the procedures employed for thorium removal, sorption by natural sorbents like zeolites and bentonites exhibits a series of advantages including high sorption capacities, high active surface, low cost, and widespread availability. Many examples of environmental remediation utilizing aluminosilicate sorbents entail the treatment of highly acidic wastewater. Most notably in the cases of ore mining and milling, high volumes of acidic liquid waste (tailings) are produced. When in contact with such media, zeolites can undergo structural changes, like dealumination or alteration of surface characteristics, which then affect the materials' sorption properties [5–8].

Moreover, the iron oxyhydroxides are a group of porous Fe(III) and Fe(II) compounds with oxide and/or hydroxide groups in their crystal lattice. In this category some of the most common iron minerals in soil substrates like ferrihydrite, goethite, magnetite, etc. are included. A multitude of applications of these compounds have been reported due to their useful chemical, structural, and physical properties, including sorption of toxic and radioactive elements [9, 10].

To the best of our knowledge, the studies related to thorium sorption using aluminosilicate materials are quite limited, especially where acid pretreatment or

modification by iron compounds is concerned [3–6]. The scope of the present work was to evaluate the effect that the iron oxyhydroxide introduction in the crystal matrix and acid pretreatment caused the sorption properties of the precursor material regarding thorium removal. Natural and modified sorbents were characterized by FTIR, XRD before and after thorium loading, their pH_{pzc} and BET surface area were calculated, and the nature of the oxyhydroxides produced was investigated. Isotherm, kinetic, and thermodynamic studies were carried out, accompanied by data fitting to theoretical models.

MATERIALS AND METHODS

Natural zeolite from Petrota region in Thrace, Greece was acquired in its powder form, which was then sieved and separated into fractions of different grain size. In all experiments described in the following sections, the fraction of particle size smaller than 50 µm was only used. All chemical reagents were of analytical grade and a water purification system (Millipore) with Elix and Milli-Q was used to provide ultra-pure water.

Modified zeolite preparation

The modified zeolite (FeZ-HCl) was prepared by acid pretreatment followed by precipitation in alkaline environment as described in the literature [11–13]. 1.85 g of precursor zeolite was suspended in a large beaker with 100 mL distilled water at room temperature and stirred for 15 min. A 50 mL solution of 0.1 mol L⁻¹ Fe(III) was prepared by dissolution of iron trichloride hexahydrate FeCl₃·6H₂O (Riedel-de Haën) and was mixed with 50 mL of 1.25 mol L⁻¹ HCl. The final solution was added to the beaker and further stirred for 40 min. Slow addition of 100 mL 1.25 mol L⁻¹ NaOH solution to create alkaline environment (pH 10-11) resulted in the immediate formation of reddish-brown precipitate, which was filtered, washed with distilled water until a neutral pH, and dried for 24 hours at 60 °C. The final iron-modified zeolite was grinded and sieved

to a particle size less than 50 μm . For comparison, the iron-modified zeolite omitting the acid pretreatment step (FeZ), as well as the pure oxyhydroxides were also prepared, according to the procedure reported in our previous study [14].

Materials characterization

The mineralogical composition of the sorbents was determined through Powder X-Ray Diffraction (pXRD) using a Rigaku MiniFlex diffractometer with Ni-filtered $\text{CuK}\alpha$ radiation. Each pulverized material was scanned with a step size of $0.01^\circ 2\theta$ in the 2θ interval of $3\text{-}90^\circ$. Attenuated Total Reflectance-Fourier Transform Infrared Spectroscopy (ATR-FTIR) was carried out in the range of $4000\text{-}400\text{ cm}^{-1}$ using a Thermo Scientific Nicolet iS20 spectrometer. The characterized materials were in contact with a diamond reflectance crystal.

The point of zero charge (pHpzc) of the sorbents was found by the pH-drift method. Solutions of $0.1\text{ mol L}^{-1}\text{ KNO}_3$ were prepared and fixed at initial pH values from 1 to 9. The sorbents were shaken for 18 hours at room temperature and the pHpzc was determined by plotting the ΔpH (difference between the initial and final pH) against the initial pH. BET surface area and volume were measured with an Autosorb-1MP, Quantachrome porosimeter by recording the adsorption/desorption of nitrogen at -196°C in the partial pressure range of 0.01 to 0.995 and after heating the samples under vacuum at 150°C .

Sorption experiments

Stock solution of 250 mg L^{-1} thorium was prepared by dissolving $\text{Th}(\text{NO}_3)_4\cdot 5\text{H}_2\text{O}$ (Merck) in bi-distilled water and was diluted to achieve the desired initial metal concentrations ($5\text{-}100\text{ mg L}^{-1}$). Sorption experiments were conducted at room temperature (ca. 298 K) using 10 mg of the sorbents contacted with 10 mL of the solutions (ratio of 1.0 g L^{-1}) in centrifuge tubes for 24 hours, enough time for the establishment of equilibrium. The liquid phase was afterwards separated by centrifugation (4000 rpm for 10 min) and filtration, and the equilibrium pH was

measured. Thorium concentrations in the supernatant solutions were determined photometrically with the Arsenazo III method at 660 nm working wavelength. The initial solution pH was adjusted to 3 by slow, dropwise addition of HNO₃ or NaOH, so as to avoid possible precipitation of thorium hydroxides occurring at higher pH values (Fig.1) [5, 15].

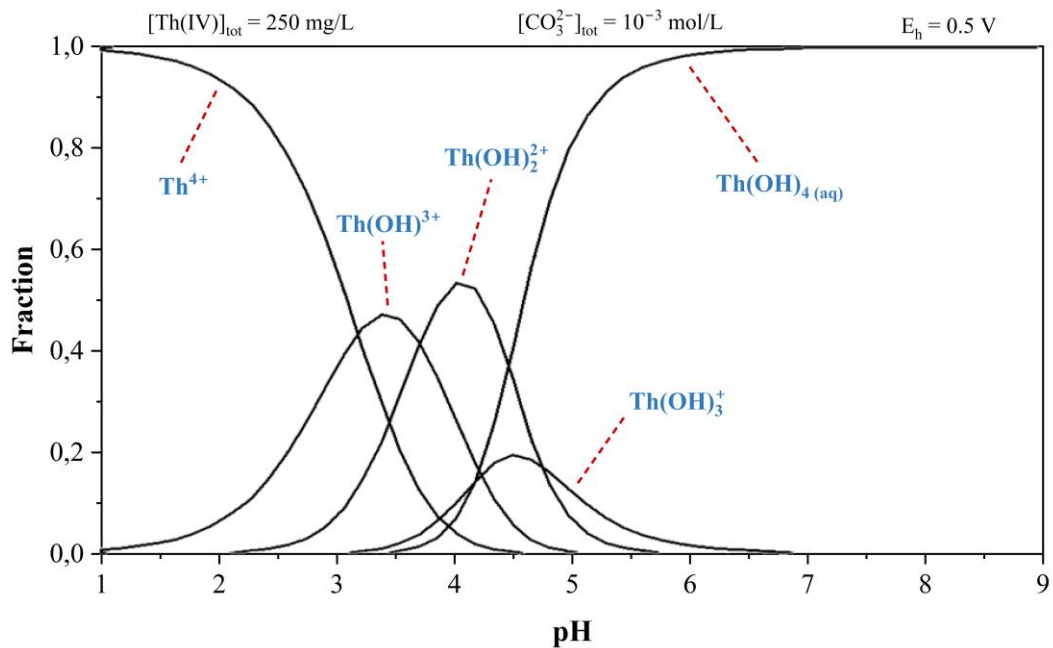


Fig. 1 Speciation diagram of ionic thorium species in aqueous solutions as calculated by the code MEDUSA.

The experimental data were then used for uptake calculations and for modelling with the Langmuir (Eq.1), which considers monolayer coverage of specific adsorption sites, and Freundlich (Eq. 2) linear isotherm, which assumes heterogeneity in the solid/liquid interface [16]. Evaluation of the linear correlation coefficients, R^2 , revealed the best-adjusted model.

$$\text{Langmuir (L)} \quad \frac{C_e}{q_e} = \frac{1}{K_L q_{max}} + \frac{1}{q_{max}} C_e \quad (1)$$

$$\text{Freundlich (F)} \quad \ln q_e = \ln K_F + \frac{1}{n} \ln C_e \quad (2)$$

In the above equations q_e and C_e are the equilibrium uptake (in mg g^{-1}) and liquid metal concentrations (in mg L^{-1}), respectively, q_{max} the maximum sorption capacity (in mg g^{-1}), K_L and K_F the Langmuir and Freundlich equilibrium constants and n , in the case of Freundlich equation, a parameter associated with the heterogeneity.

Kinetic and thermodynamic studies

The effect of contact time and temperature was investigated using stock thorium solutions of 100 mg L^{-1} concentration (at pH 3) at three different temperatures, 298, 308, and 318 K. Known amounts of the raw zeolite and each solution (with 1.0 g L^{-1} ratio) were contacted, and at predetermined time intervals between 2 and 60 min, 10 mL aliquots were drawn with a syringe, filtered, and transferred to polypropylene tubes for photometric thorium determination.

The results were afterwards fitted to the pseudo-first (PFO) and pseudo-second order (PSO) kinetic models, using the linear forms of the equations (Eq. 3 and Eq. 4). According to the PFO model, sorption is due to physical interactions and mass transfer by diffusion, while according to the PSO model, the critical step of the process may involve chemical interactions between the adsorbent and the adsorbate [17].

$$\text{PFO} \quad \ln(q_e - q_t) = \ln(q_e) - k_1 t \quad (3)$$

$$\text{PSO} \quad \frac{t}{q_t} = \frac{1}{q_e^2 k_2} + \frac{1}{q_e} t \quad (4)$$

In both previous cases, q_t (in mg g^{-1}) is the thorium uptake at time t (in min), and q_e (in mg g^{-1}) is the thorium uptake at equilibrium. The pseudo-first and pseudo-second order reaction rate constants are represented by k_1 (in min^{-1}) and k_2 (in $\text{g mg}^{-1} \text{ min}^{-1}$) respectively.

The sorption activation energy, E_a , is the amount of energy required for the reaction to occur, and can be easily calculated using the appropriate k constant, as determined by previous analysis of the kinetic data, with the Arrhenius equation (Eq. 5), where A

(same units as k) is the Arrhenius factor, R ($=8.314 \text{ J mol}^{-1} \text{ K}^{-1}$) is the universal gas constant, and T (in K) the absolute temperature.

$$\ln k = \ln A - \frac{E_a}{RT} \quad (5)$$

Finally, thermodynamic parameters were calculated. The Gibbs free energy change, ΔG° (in J mol^{-1}), is related to the spontaneity of the sorption and is given by Eq. 6, in which $K_D=q_e/C_e$ (L g^{-1}) is the distribution coefficient at equilibrium [18].

$$\Delta G^\circ = -RT \ln K_D \quad (6)$$

The enthalpy change, ΔH° (in J mol^{-1}), which determines the exothermic or endothermic character of the reaction, and the entropy change, ΔS° (in $\text{J mol}^{-1} \text{ T}^{-1}$), which is a measure of the degree of disorder in the system, can be calculated using the van't Hoff equation (Eq. 7).

$$\ln K_D = \frac{\Delta S^\circ}{R} - \frac{\Delta H^\circ}{R} \frac{1}{T} \quad (7)$$

RESULTS AND DISCUSSION

Materials characterization

The FTIR spectra of the raw and loaded sorbents are presented in Fig. 2. The pattern observed for the natural zeolite is characteristic for HEU-type zeolites [19–21]. The broad band at approximately 3390 cm^{-1} is attributed to stretching O–H vibrations of water molecules and hydroxyl groups while the band at 3616 cm^{-1} is due to surface Si–OH and Al–OH groups of the lattice. The respective bending O–H vibrations can be seen at 1630 cm^{-1} . Typical aluminosilicate bands are detected at 1005 , 792 , and 585 cm^{-1} corresponding to the asymmetric stretching vibrations of both the zeolitic tetrahedra (T–O–T) and similar vibration modes of possible mineral impurities (quartz,

feldspars), the symmetrical internal stretching vibrations of O–T–O bonds, and finally vibrations related to the pore structure of HEU-type zeolites.

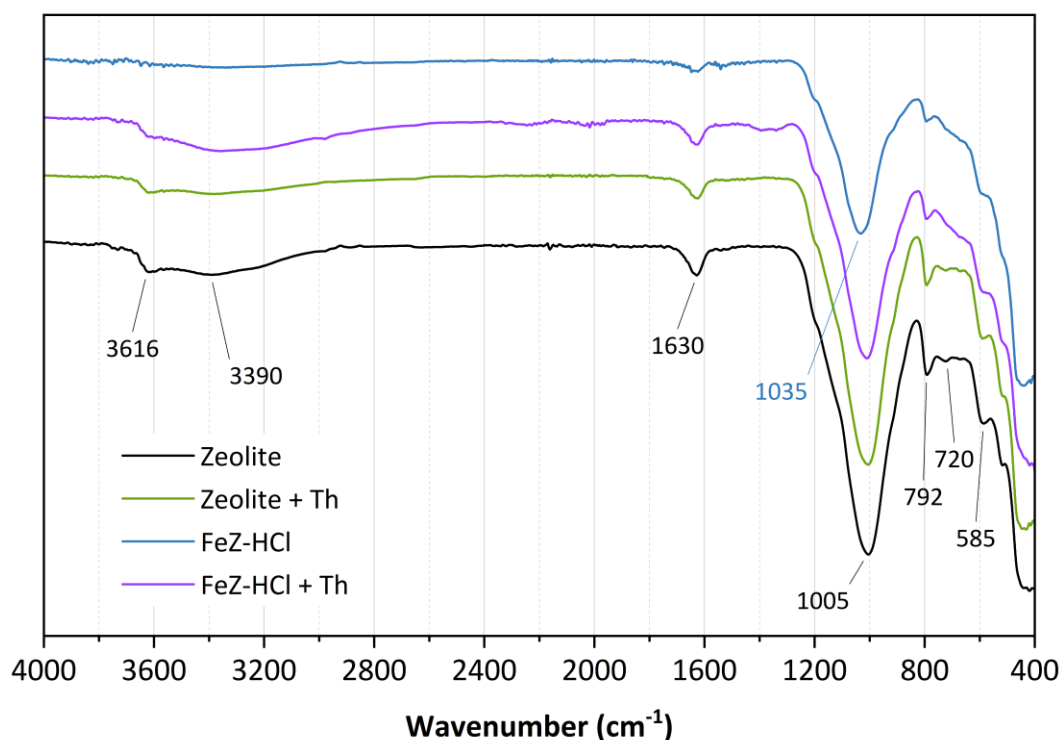


Fig. 2 FTIR spectra of the raw (Zeolite) and modified zeolites (FeZ-HCl) before and after thorium loading.

Acid treatment and the introduction of iron oxyhydroxides did not alter the peak pattern of the precursor material pointing to retention of the basic zeolite structure after modification [13, 21, 22]. However, minor changes in the intensity and position of the main band can be observed. Specifically, the shift towards higher wavenumbers (1035 cm⁻¹) could be explained by the interaction between newly-introduced Fe–O groups of the oxyhydroxides and surface tetrahedra, as well as the acid pretreatment step. A high concentration of H⁺ ions can attack and break Si–O–Al bonds, leading to dealumination and removal of Al³⁺ from the lattice. The stronger Si–O bonds are detected in higher wavenumbers [23]. Thorium sorption did not affect band position and number for both materials.

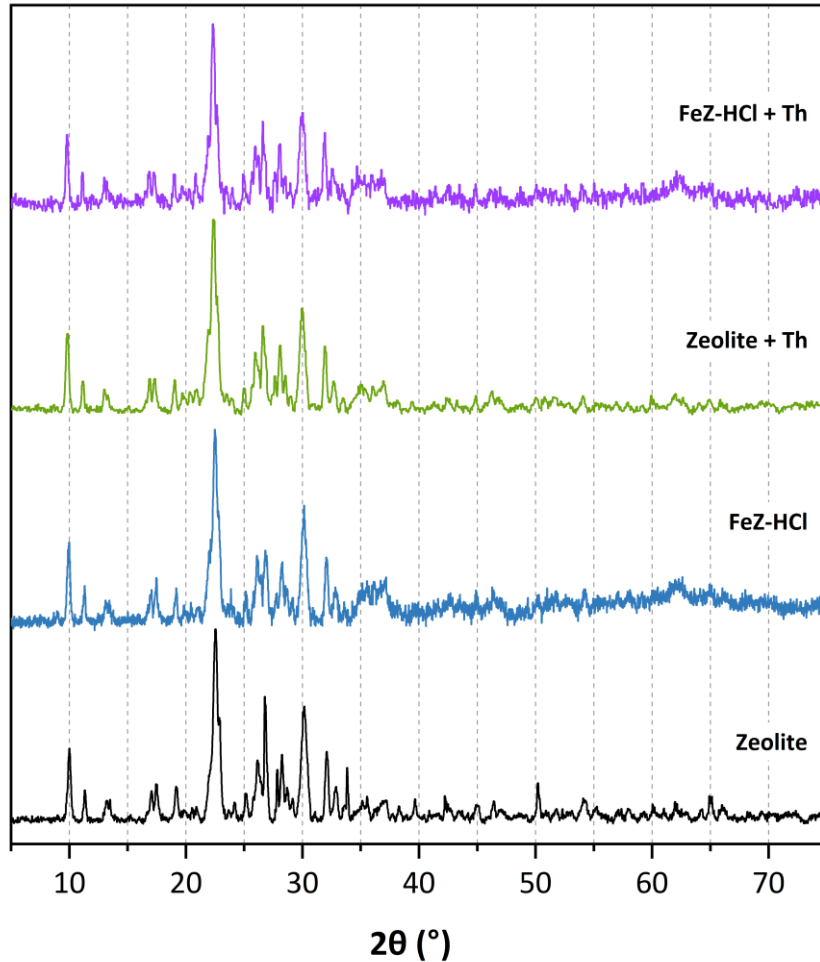


Fig. 3 pXRD patterns of raw zeolite and iron-modified zeolite, before and after uranium sorption.

The powder XRD pattern of the zeolite (Fig. 3) reveals the characteristic clinoptilolite diffraction peaks at $2\theta=10.01, 11.33, 22.55, 30.16^\circ$ which correspond to the (020), (200), (400), (151) planes. The natural zeolite consisted of up to 89% HEU-type zeolite, but small quantities of impurities like quartz, feldspars, clay, and mica were also present, as indicated by the diffraction peaks at $2\theta=26.77$ and 28.27° [22, 23]. In the modified material (FeZ-HCl) the clinoptilolite peaks remained unchanged in number and position, confirming the zeolite structure without any new mineral phases. However, the material has a more amorphous character, induced by acid treatment and partial dissolution of the lattice [23]. Thorium sorption did not alter the basic peak pattern for both materials, meaning that no new mineral phases were created. Minor shifts in the range of 0.2° to lower 2θ values indicate lattice expansion, related to thorium binding.

Table 1 shows the results of the BET and pHpzc methods. The point of zero charge has decreased by almost 2.5 units in the modified sorbent. As revealed by the pHpzc curves (Fig. 4) surface charge characteristics are different for FeZ-HCl. Similar results have been observed by other researchers and were attributed to a possible positively charged film of Al^{3+} ions or otherwise by the more intense H^+ adsorption due to defects by dealumination and partial amorphization [23, 26].

Table 1 Surface areas and pore volumes calculated with the BET method, and the point of zero charge of the evaluated materials.

Material	S_{BET} (m^2/g)	S_{micro} (m^2/g)	V_{BET} (cm^3/g)	V_{micro} (cm^3/g)	pHpzc
Zeolite	32	9	0.106	0.004	7.00
FeZ-HCl	90	13	0.133	0.006	4.60

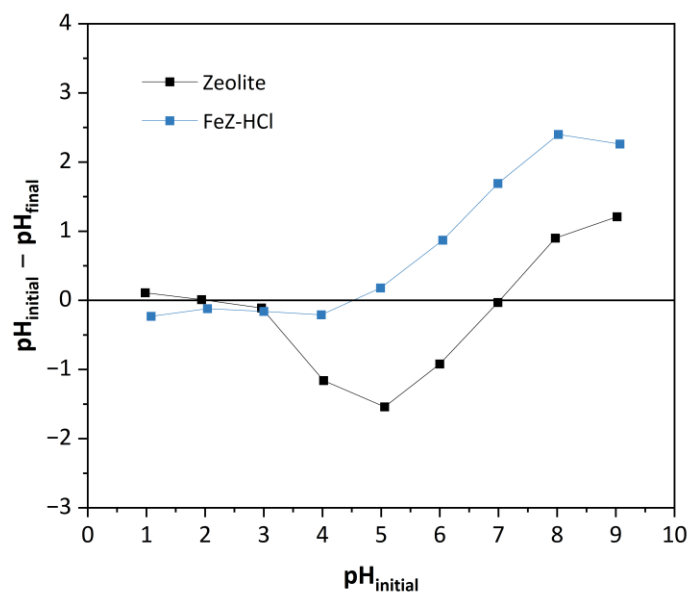


Fig. 4 N_2 adsorption-desorption isotherms and pore size distribution calculated according to the NLDFT model for the raw and iron-modified zeolites.

Concerning BET measurements, it is obvious that both surface area as well as volume have been significantly enhanced post modification. The amorphous nature of the

surface-deposited iron oxyhydroxide layer results in the creation of vacant space among the randomly precipitated particles, thus enhancing the surface area [21, 26, 27]. This is further confirmed by the pore size distribution (Fig. 5) showing a large increase in the pores with diameters in the region of 1-4 nm. The increase in total volume can be attributed to the structural changes caused by acid treatment.

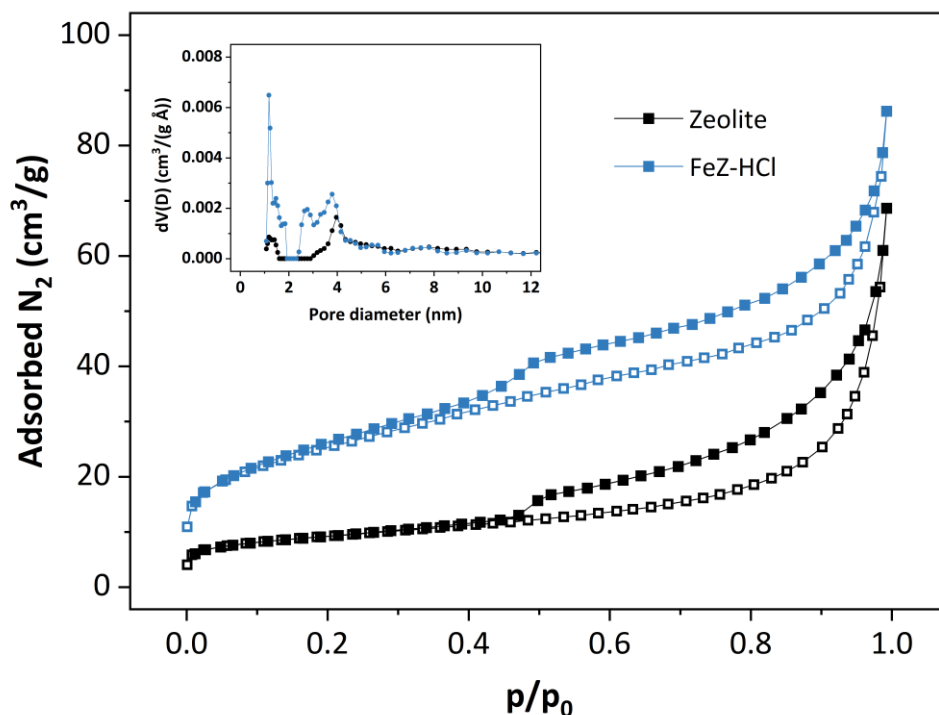


Fig. 5 N₂ adsorption-desorption isotherms and pore size distribution calculated according to the NLDFT model for the raw and iron-modified zeolites.

A detailed presentation of the characterization results for FeZ and the pure iron oxyhydroxides is given in our previous study [14], where it was observed that even without acid pretreatment, iron modification had in general similar effects as discussed above. Concerning the nature of iron oxyhydroxides produced, it was concluded that they were a mixture consisting mostly of amorphous ferrihydrite co-existing with small amounts of low-crystallinity goethite (α -FeOOH).

Thorium sorption

Fig. 6 displays the thorium sorption isotherms on natural and modified zeolites, which demonstrate the change of uptake values as a function of the equilibrium metal

concentration. These data can afterwards give information on the phenomenon and help elucidate the sorption mechanism. A significant decrease in the amount of thorium sorbed can be observed concerning the modified materials. At initial concentration equal to 25 mg L^{-1} , almost 70% of the metal has been adsorbed onto the natural zeolite, compared to the 55% and 32% removed by the FeZ and FeZ-HCl modified zeolites respectively.

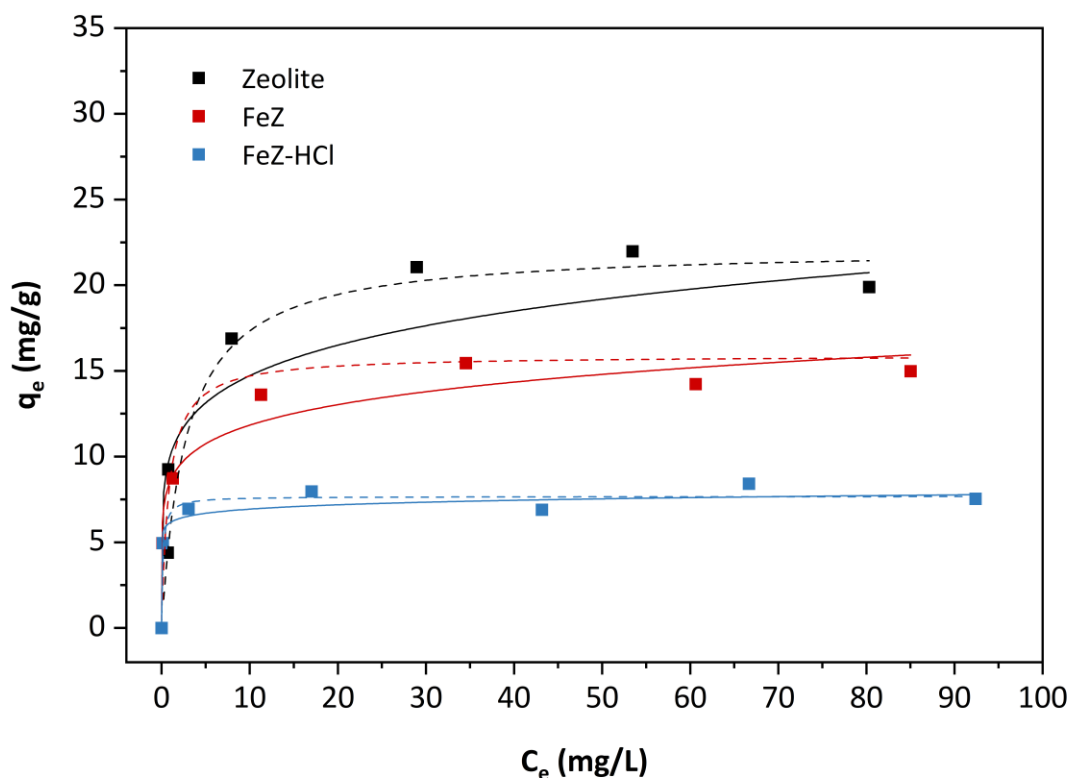


Fig. 6 Thorium sorption isotherms onto the raw and modified zeolites (dosage: 1 g L^{-1} , T: 295 K). Solid lines depict the Freundlich fitting and dashed lines the Langmuir fitting.

As it is known, the zeolitic framework hosts mainly negative charge owing to the $[\text{AlO}_4]^{5-}$ tetrahedra, which is then compensated by exchangeable cations like Na^+ , Ca^{2+} , K^+ , Mg^{2+} [20, 24]. As a result, cations like Th^{4+} , $[\text{Th}(\text{OH})]^{3+}$, $[\text{Th}(\text{OH})_2]^{2+}$ which dominate in acidic media (Fig. 1) readily sorb on the material's surface. However, since the initial solution pH was quite acidic, the competition for active site binding between the cationic thorium species and H^+ is high.

The further decrease in uptake in the case of the modified materials can be explained by considering the following two points. Firstly, researchers have observed a decrease

in porosity in iron oxyhydroxide-treated sorbents [28] which in turn deters the large size thorium ions from reaching the active binding sites. This is supported by BET surface area results, showing a sharp increase in small diameter micropores. Secondly, concerning specifically FeZ-HCl the dealumination process described before has affected surface charge characteristics. As a result, the electrostatic repulsion is higher and inhibits the approach of thorium ionic species to the surface.

Table 2 contains fitting data of the experimental results for the Langmuir and Freundlich models. As can be seen for all investigated materials, the Langmuir isotherm shows a higher correlation factor, meaning that the sorption proceeds via the monolayer coverage described by the model.

Table 2 Parameters of the Langmuir and Freundlich models for thorium adsorption.

Material	Langmuir			Freundlich		
	K_L (L mg ⁻¹)	q_{max} (mg g ⁻¹)	R^2	K_F	$1/n$	R^2
Zeolite	0.9355	20.88	0.9948	7.4940	0.2722	0.8052
FeZ	1.7846	14.90	0.9983	7.9526	0.1649	0.9466
FeZ-HCl	2.7845	7.74	0.9911	5.9787	0.0670	0.7765

There are few literature-works concerning thorium sorption on natural aluminosilicate sorbents under different conditions (e.g. pH, concentration, dosage) [3–6, 29, 30]. Even more limited is the number of works examining sorption on oxyhydroxide-modified zeolites or bentonites [31–33]. In most cases the authors have concluded that the sorption mechanism includes mainly the formation of surface complexes, especially when iron oxyhydroxides are present, while ion exchange can also take place. The results of the current study are compared to the literature works in Table 3.

Table 3 Literature data for thorium sorption on natural and iron-modified aluminosilicates, as well as on iron oxyhydroxides.

Material	q_{\max} (mg g^{-1})	Concentration range (mg L^{-1})	pH	Dosage (g L^{-1})	Reference
Clinoptilolite	19.89	5-100	3	1.0	This work
ZSM-5	2.55	0-2.78	3.6	2.4	[3]
NKF-6	64.97	10-33	3	0.45	[4]
Activated bentonite	26.22	1.76-23.2	2.5	0.3	[5]
Na-clinoptilolite	175	154-3870	4	10.0	[29]
Phillipsite/chabazite tuff	21.9	5-40	3	1.0	[30]
Na-bentonite	41.24	1.2-235	6.2	2.5	[31]
Clinoptilolite/FeO(OH)s	14.99	5-100	3	1.0	This work
Clinoptilolite/FeO(OH)s/HCl	7.54	5-100	3	1.0	This work
Na-bentonite/Fe ₃ O ₄	31.34	1.2-235	6.2	2.5	[31]
Ferrihydrite/Fe ₃ O ₄	0.016/0 .024	0.255	2.9	10	[32]
Fe ₃ O ₄	4.64	0.25-29.5	2.6	0.6	[33]

Effect of contact time and temperature

The effect of contact time and temperature on thorium sorption on the natural zeolite is depicted in Fig. 7. Equilibrium conditions are achieved very fast, within the first 20 min of contact time, which is generally observed if ion exchange takes place [34]. By increasing the solution temperature, adsorption is strengthened and thus, the reaction is endothermic. In the literature, thorium sorption on aluminosilicate materials has mostly been found to be an endothermic phenomenon [3–6], attributed to the increased degree of hydrolysis and easier elimination of the hydration spheres at higher temperatures [33], but it has also been reported as exothermic [30, 31].

Kinetic results from the three different temperatures are best fitted to the pseudo-second order (PSO) model (Table 4), which signifies that the reaction-controlling step of adsorption may be of chemical nature. The activation energy calculated by the Arrhenius equation (Fig. 8a) is also indicative of a complex mechanism. Complex processes consist of separate reaction steps each having a certain activation energy. This way, the negative value of the overall experimentally observed activation energy can be explained if it is considered that an increase in temperature has a different

effect on each of these individual steps. Negative activation energies of metal sorption of comparative magnitude have also been reported in other works [35, 36].

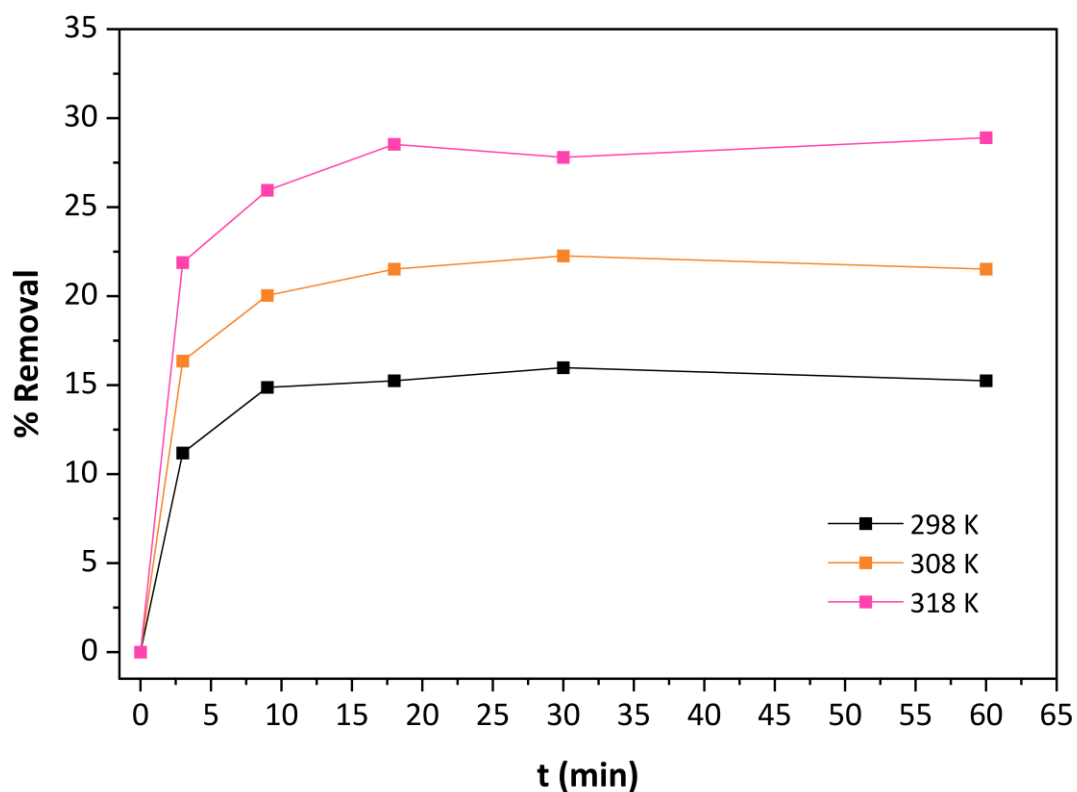


Fig. 7 Effect of contact time and temperature on thorium sorption onto the natural zeolite (dosage: 1 g L⁻¹, C₀: 100 mg L⁻¹)

Table 4 Kinetic parameters for thorium sorption at different temperatures and activation energy as calculated by modeling of experimental data.

T (K)	Pseudo-First Order			Pseudo-Second Order			E _a (kJ mol ⁻¹)
	k ₁ (min ⁻¹)	q _e (mg g ⁻¹)	R ²	k ₂ (g mg ⁻¹ min ⁻¹)	q _e (mg g ⁻¹)	R ²	
298	0.4258	15.43	0.9707	0.1613	15.51	0.9991	-62.99
308	0.4657	21.46	0.9164	0.0819	22.27	0.9992	
318	0.4969	27.93	0.8744	0.0325	29.33	0.9997	

Finally, the van't Hoff diagram (Fig. 8b) was used to determine the thermodynamic parameters ΔG° , ΔH° , and ΔS° after calculating the distribution coefficients K_D at

equilibrium (Table 5). As can be seen, the phenomenon is spontaneous (due to the negative values of the Gibbs free energy), is confirmed to be endothermic (due to the positive enthalpy), and leads to increased disorder in the solid/liquid interface (due to the positive entropy).

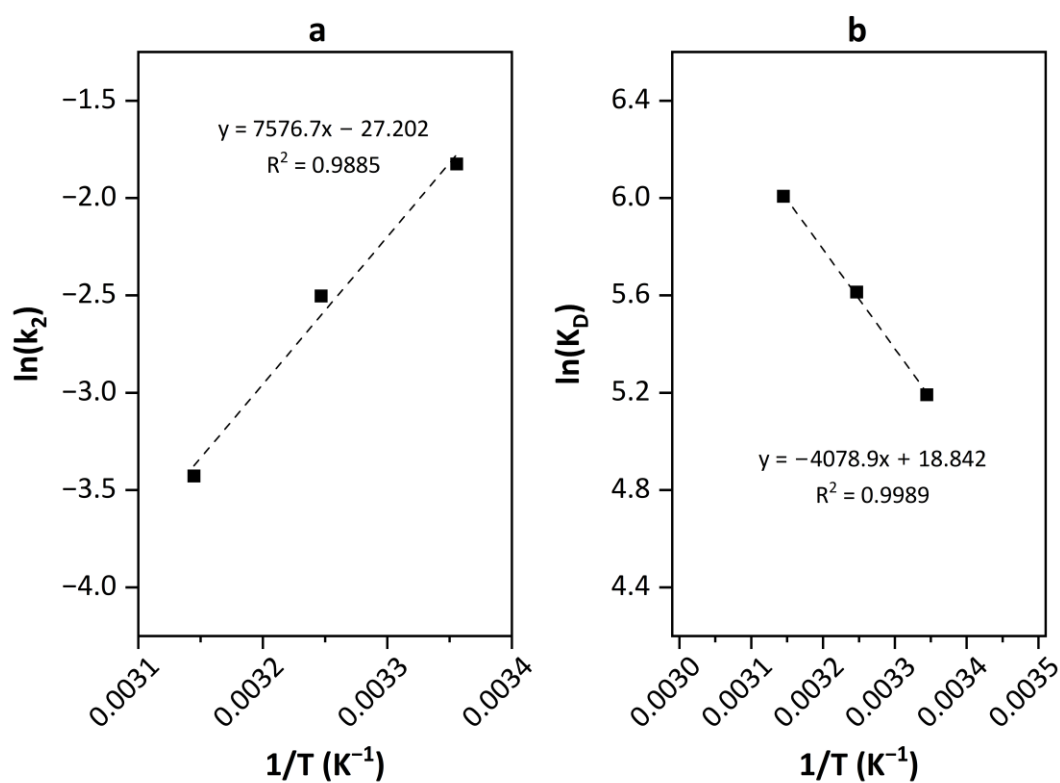


Fig. 8 Arrhenius plot (a) and van't Hoff diagram (b) for the adsorption of thorium on zeolite

Table 5 Distribution coefficients and thermodynamic parameters of thorium sorption on zeolite.

T (K)	K_D ($mL\ g^{-1}$)	ΔG° ($kJ\ mol^{-1}$)	ΔH° ($kJ\ mol^{-1}$)	ΔS° ($kJ\ mol^{-1}\ K^{-1}$)
298	179.9	-12.9	33.91	0.157
308	274.2	-14.4		
318	406.5	-15.9		

CONCLUSIONS

- A natural zeolite was successfully modified with hydrochloric acid and/or iron oxyhydroxides using a simple and fast precipitation by base method. The oxyhydroxides were identified as mostly amorphous ferrihydrite coexisting with poorly crystalline α -FeOOH.
- Consideration of FTIR, XRD, N₂-BET, and pH_{zpc} revealed that after modification, the fundamental zeolite structure was preserved, but charge and surface characteristics were greatly affected.
- Thorium sorption was lower on the modified zeolites possibly due to greater electrostatic repulsion and limited access of Th(IV) ions to the active binding sites.
- Isotherm fitting data showed better correlation with the Langmuir theoretical model, indicating monolayer coverage.
- Evaluation of kinetic and thermodynamic parameters revealed a complex phenomenon, fitted to the pseudo-second order reaction model with a spontaneous, endothermic character.

Acknowledgements

The authors would like to thank Ms. Eleftheria Kapashi for the XRD measurements and Prof. K. Triantafyllidis (Chemistry Department, AUTH) for the results of the BET technique.

References

1. Miloš René, "Nature, Sources, Resources, and Production of Thorium," in InTech eBooks, 2017, <https://doi.org/10.5772/intechopen.68304>.

2. Charmaine D. Tutson and Anne E.V. Gorden, "Thorium Coordination: A Comprehensive Review Based on Coordination Number," *Coordination Chemistry Reviews* 333 (November 2016): 27–43, <https://doi.org/10.1016/j.ccr.2016.11.006>.
3. Qing-Hua Xu, Duo-Qiang Pan, and Wang-Suo Wu. "Effects of pH, Ionic Strength, Humic Substances and Temperature on Th(IV) Sorption Onto ZSM-5." *Journal of Radioanalytical and Nuclear Chemistry* 305, no. 2 (March 2015): 535–41. <https://doi.org/10.1007/s10967-015-4007-7>.
4. Jian Wang, Zhongshan Chen, Wanying Chen, Yinshi Li, Yunchao Wu, Jun Hu, Ahmed Alsaedi, Njud S. Alharbi, Junfei Dong, and Wensheng Linghu. "Effect of pH, Ionic Strength, Humic Substances and Temperature on the Sorption of Th(IV) Onto NKF-6 Zeolite." *Journal of Radioanalytical and Nuclear Chemistry* 310, no. 2 (May 2016): 597–609. <https://doi.org/10.1007/s10967-016-4868-4>.
5. Zhuoxin Yin, Duoqiang Pan, Peng Liu, Hanyu Wu, Zhan Li, and Wangsuo Wu. "Sorption Behavior of Thorium(IV) Onto Activated Bentonite." *Journal of Radioanalytical and Nuclear Chemistry* 316, no. 1 (February 2018): 301–12. <https://doi.org/10.1007/s10967-018-5716-5>.
6. Pankaj Sharma and Radha Tomar, "Sorption Behaviour of Nanocrystalline MOR Type Zeolite for Th(IV) and Eu(III) Removal From Aqueous Waste by Batch Treatment," *Journal of Colloid and Interface Science* 362, no. 1 (June 2011): 144–56, <https://doi.org/10.1016/j.jcis.2011.06.030>.
7. Marin Senila and Oana Cadar, "Modification of Natural Zeolites and Their Applications for Heavy Metal Removal From Polluted Environments: Challenges, Recent Advances, and Perspectives," *Heliyon* 10, no. 3 (February 2024): e25303, <https://doi.org/10.1016/j.heliyon.2024.e25303>.
8. Fazila Younas et al., "Environmental Applications of Natural and Surface-Modified Zeolite," in *Advances in Material Research and Technology*, 2023, 373–96, https://doi.org/10.1007/978-981-99-2544-5_17.

9. Meiqing Shi et al., "Recent Progress in Understanding the Mechanism of Heavy Metals Retention by Iron (Oxyhydr)Oxides," *The Science of the Total Environment* 752 (August 2020): 141930, <https://doi.org/10.1016/j.scitotenv.2020.141930>.
10. Dien Li and Daniel I. Kaplan, "Sorption Coefficients and Molecular Mechanisms of Pu, U, Np, Am and Tc to Fe (Hydr)Oxides: A Review," *Journal of Hazardous Materials* 243 (September 2012): 1–18, <https://doi.org/10.1016/j.jhazmat.2012.09.011>.
11. Hossein Jahangirian et al., "Green Synthesis of Zeolite/Fe₂O₃ Nanocomposites: Toxicity & Cell Proliferation Assays and Application as a Smart Iron Nanofertilizer," *International Journal of Nanomedicine* 15 (February 2020): 1005–20, <https://doi.org/10.2147/ijn.s231679>.
12. E. N. Bakatula, R. Molaudzi, P. Nekhunguni, and H. Tutu. "The Removal of Arsenic and Uranium From Aqueous Solutions by Sorption Onto Iron Oxide-Coated Zeolite (IO CZ)." *Water Air & Soil Pollution* 228, no. 1 (December 2016). <https://doi.org/10.1007/s11270-016-3190-7>.
13. Xiaohui Yang, Bing Yan, Yi Liu, Feng Zhou, Dan Li, and Zuhua Zhang. "Gamma-FeOOH Based Hierarchically Porous Zeolite Monoliths for As(V) Removal: Characterisation, Adsorption and Response Surface Methodology." *Microporous and Mesoporous Materials* 308 (August 2020): 110518. <https://doi.org/10.1016/j.micromeso.2020.110518>.
14. Filippou Karantoumanis, Panagiotis Tsamos, and Fotini Noli. "Application of a Greek zeolite embedded with Fe-oxyhydroxides for uranium retention in aqueous solutions." *Water, Air, & Soil Pollution* 236, no. 5 (April 2025) <https://doi.org/10.1007/s11270-025-07923-1>.
15. MEDUSA (Make Equilibrium Diagrams Using Sophisticated Algorithms) (1983) I. Puigdomènech, INPUT, SED, and PREDOM: computer programs drawing equilibrium diagrams. Report TRITA-OK-3010, Royal Institute of Technology (KTH), Dept. Inorg. Chemistry, Stockholm, Sweden.

16. Jianlong Wang and Xuan Guo, "Adsorption Isotherm Models: Classification, Physical Meaning, Application and Solving Method," *Chemosphere* 258 (June 2020): 127279, <https://doi.org/10.1016/j.chemosphere.2020.127279>.
17. Jianlong Wang and Xuan Guo, "Adsorption Kinetic Models: Physical Meanings, Applications, and Solving Methods," *Journal of Hazardous Materials* 390 (January 2020): 122156, <https://doi.org/10.1016/j.jhazmat.2020.122156>.
18. Kailas Mahadeo Doke and Ejazuddin M. Khan, "Adsorption Thermodynamics to Clean up Wastewater; Critical Review," *Reviews in Environmental Science and Bio/Technology* 12, no. 1 (February 27, 2012): 25–44, <https://doi.org/10.1007/s11157-012-9273-z>.
19. K. Byrappa and B. V. Suresh Kumar, "Characterization of zeolites by infrared spectroscopy." *Asian Journal of Chemistry* 19, no. 6 (2007): 4933–5.
20. K. Elaiopoulos, Th. Perraki, and E. Grigoropoulou, "Monitoring the Effect of Hydrothermal Treatments on the Structure of a Natural Zeolite Through a Combined XRD, FTIR, XRF, SEM and N₂-porosimetry Analysis," *Microporous and Mesoporous Materials* 134, no. 1–3 (May 2010): 29–43, <https://doi.org/10.1016/j.micromeso.2010.05.004>.
21. Maria K. Doula, "Synthesis of a clinoptilolite–Fe System With High Cu Sorption Capacity," *Chemosphere* 67, no. 4 (December 2006): 731–40, <https://doi.org/10.1016/j.chemosphere.2006.10.072>.
22. Marin Ugrina, Teja Čeru, Ivona Nuić, and Marina Trgo. "Comparative Study of Mercury(II) Removal From Aqueous Solutions Onto Natural and Iron-Modified Clinoptilolite Rich Zeolite." *Processes* 8, no. 11 (November 2020): 1523. <https://doi.org/10.3390/pr8111523>.
23. Srdjan Matijasevic, Snezana Zildzovic, Jovica Stojanovic, Marija Djosic, Jelena Nikolic, Mirjana Stojanovic, and Nebojsa Labus. "Removal of Uranium (VI) From Aqueous Solution by Acid Modified Zeolites." *Zastita Materijala* 57, no. 4 (January 2016): 551–58. <https://doi.org/10.5937/zasmat1604551m>.

24. Anestis Filippidis, Nikolaos Kantiranis, and Ananias Tsirambides. "The mineralogical composition of Thrace zeolitic rocks and their potential use as feed additives and nutrition supplements." *Bulletin of the Geological Society of Greece* L (May 2016): 1820–8.
25. Sema Akyalcin, Levent Akyalcin, and Ecem Ertugrul, "Modification of Natural Clinoptilolite Zeolite to Enhance Its Hydrogen Adsorption Capacity," *Research on Chemical Intermediates* 50, no. 3 (January 2024): 1455–73, <https://doi.org/10.1007/s11164-023-05212-2>.
26. Jolanta Cieřla, Wojciech Franus, Małgorzata Franus, Karolina Kedziora, Justyna Gluszczyk, Justyna Szerement, and Grzegorz Jozefaciuk. "Environmental-Friendly Modifications of Zeolite to Increase Its Sorption and Anion Exchange Properties, Physicochemical Studies of the Modified Materials." *Materials* 12, no. 19 (September 2019): 3213. <https://doi.org/10.3390/ma12193213>.
27. Yu. S. Dzyazko, L. M. Rozhdestvenska, K. O. Kudelko, I. V. Fedina, L. M. Ponomaryova, G. M. Nikovska, and O. G. Dzyazko. "Hydrated Iron Oxide Embedded to Natural Zeolite: Effect of Nanoparticles and Microparticles on Sorption Properties of Composites." *Water Air & Soil Pollution* 233, no. 6 (May 2022). <https://doi.org/10.1007/s11270-022-05681-y>.
28. P. D. Bhalara, D. Punetha, and K. Balasubramanian, "Kinetic and Isotherm Analysis for Selective Thorium(IV) Retrieval From Aqueous Environment Using Eco-friendly Cellulose Composite," *International Journal of Environmental Science and Technology* 12, no. 10 (October 2014): 3095–3106, <https://doi.org/10.1007/s13762-014-0682-0>.
29. Yones Khazaei, Hossein Faghihian, and Mahdi Kamali, "Removal of Thorium From Aqueous Solutions by Sodium Clinoptilolite," *Journal of Radioanalytical and Nuclear Chemistry* 289, no. 2 (April 2011): 529–36, <https://doi.org/10.1007/s10967-011-1100-4>.

30. Mona Al-Shaybe and Fawwaz Khalili, "Adsorption of Thorium (IV) and Uranium (VI) by Tulul al-Shabba Zeolitic Tuff, Jordan," *Jordan Journal of Earth and Environmental Sciences* 2, (December 2009): 108–19.
31. Abdelkader Miraoui and Mohamed Amine Didi, "Thorium(IV) Sorption Onto Sodium Bentonite and Magnetic Bentonite," *European Chemical Bulletin* 4, no. 11 (December 2015): 512–21, <https://doi.org/10.17628/ECB.2015.4.512>
32. I. Rojo, F. Seco, M. Rovira, J. Giménez, G. Cervantes, V. Martí, and J. De Pablo. "Thorium Sorption Onto Magnetite and Ferrihydrite in Acidic Conditions." *Journal of Nuclear Materials* 385, no. 2 (December 2008): 474–78. <https://doi.org/10.1016/j.jnucmat.2008.12.014>.
33. Ping Li, Xiangxian Ma, Hong Li, Shicheng Li, Hanyu Wu, Di Xu, Guodong Zheng, and Qiaohui Fan. "Sorption Mechanism of Th(IV) at Iron Oxyhydroxide (IOHO)/Water Interface: Batch, Model and Spectroscopic Studies." *Journal of Molecular Liquids* 241 (June 2017): 478–85. <https://doi.org/10.1016/j.molliq.2017.06.048>.
34. W. Mozgawa and T. Bajda, "Spectroscopic Study of Heavy Metals Sorption on Clinoptilolite," *Physics and Chemistry of Minerals* 31, no. 10 (December 2004): 706–13, <https://doi.org/10.1007/s00269-004-0433-8>.
35. S. Hojati and A. Landi, "Kinetics and Thermodynamics of Zinc Removal From a Metal-plating Wastewater by Adsorption Onto an Iranian Sepiolite," *International Journal of Environmental Science and Technology* 12, no. 1 (October 2014): 203–10, <https://doi.org/10.1007/s13762-014-0672-2>.
36. M. Hamdi Karaoğlu, Şule Zor, and Mehmet Uğurlu, "Biosorption of Cr(III) From Solutions Using Vineyard Pruning Waste," *Chemical Engineering Journal* 159, no. 1–3 (March 2010): 98–106, <https://doi.org/10.1016/j.cej.2010.02.047>.